ISSN 1674-1056
http://cpb.iphy.ac.cn
http://iopscience.iop.org/cpb
中国物理 B
Chinese Physics
中国物理
Chinese Physics B

Relativistic *R*-matrix calculations for *L*-shell photoionization cross sections of C II

Lu-You Xie(颉录有), Qian-Qian Man(满倩倩), Jiang-Guo Wang(王建国), Yi-Zhi Qu(屈一至), Chen-Zhong Dong(董晨钟)

Citation: Chin. Phys. B . 2018, 27(8): 083201. **doi:** 10.1088/1674-1056/27/8/083201

Journal homepage: http://cpb.iphy.ac.cn; http://iopscience.iop.org/cpb

What follows is a list of articles you may be interested in

Pressure-broadened atomic Li(2s-2p) line perturbed by ground neon atoms in the spectral wings and core

Sabri Bouchoucha, Kamel Alioua, Moncef Bouledroua

Chin. Phys. B . 2017, 26(7): 073202. **doi:** 10.1088/1674-1056/26/7/073202

Dirac R-matrix calculations of photoionization cross sections of Ni XII and atomic structure data of Ni XIII

R T Nazir, M A Bari, M Bilal, S Sardar, M H Nasim, M Salahuddin

Chin. Phys. B . 2017, 26(2): 023102. **doi:** 10.1088/1674-1056/26/2/023102

Influence of the interaction volume on the kinetic energy resolution of a velocity map imaging spectrometer

Peng Zhang(张鹏), Zheng-Peng Feng(冯正鹏), Si-Qiang Luo(罗四强), Zhe Wang(王哲)

Chin. Phys. B . 2016, 25(3): 033202. **doi:** 10.1088/1674-1056/25/3/033202

Relativistic R-matrix calculations for L-shell photoionization cross sections of C II*

Lu-You Xie(颉录有)[1,†], Qian-Qian Man(满倩倩)[1], Jian-Guo Wang(王建国)[2], Yi-Zhi Qu(屈一至)[3], and Chen-Zhong Dong(董晨钟)[1]

[1] *Key Laboratory of Atomic and Molecular Physics & Functional Materials of Gansu Province, College of Physics and Electronic Engineering, Northwest Normal University, Lanzhou* 730070, *China*

[2] *Key Laboratory of Computational Physics, Institute of Applied Physics and Computational Mathematics, Beijing* 100088, *China*

[3] *College of Material Sciences and Opto-electronic Technology, University of the Chinese Academy of Sciences, Beijing* 100049, *China*

(Received 30 March 2018; revised manuscript received 17 May 2018; published online 10 July 2018)

The photoionization cross section of the ground state $2s^22p\ ^2P^o_{1/2}$ and the first excited state $2s^22p^2P^o_{3/2}$ of C II ions are systematically calculated using the fully relativistic R-matrix code DARC. The detailed resonances are presented and identified for the photon energy ranging from threshold (24.38 eV) up to 41.5 eV where the L-shell (2p, 2s) photoionization process is dominant. In the calculations, the relativistic effect and electronic correlation effect are well considered. It is found that the relativistic effect is very important for the light atomic system CII, which accounts for experimentally observed fine structure resonance peaks. A careful comparison is made between the present results and the experimental values, and also other theoretical data available in the literature, showing that good agreement is obtained for the resonance peaks.

Keywords: photoionization cross section, relativistic R-matrix method, C II

PACS: 32.80.–t, 31.15.am **DOI:** 10.1088/1674-1056/27/8/083201

1. Introduction

Study of the photoionization (PI) process of atomic systems provides the opportunity to investigate the dynamic interplay between many-body electron–electron correlations and the relativistic effects.[1,2] Besides its fundamental significance, the PI cross section is also of vital importance as applied data in atmospheric physics, astrophysics, and plasma and tokomak researches.[3–5] Much theoretical and experimental effort has been devoted for over three decades to the study of PI cross sections. Among these theoretical researches, the most comprehensive studies have been carried out for a large number of relatively light atoms and ions of astrophysical relevance by using the close-coupling R-matrix method in the frame work of the Opacity Project,[6,7] the Iron,[8] and the RmaX projects.[9] However, many of those calculations have been performed in the framework of non-relativistic theory, and the relativistic effects, for example, the spin–orbit split cannot be included. Numbers of high-resolution and state-selective experimental measurements have been carried out with synchrotron-radiation sources,[10,11] which provide accurate data on ionic structure and PI cross sections, especially the resonance peaks and guidance to the development of theoretical models. To explain these high-resolution experiments, both elaborate configuration interaction (CI) and fully relativistic effects should be considered.

C II is an important ion in astrophysical sources, such as the interstellar medium. Study of accurate features of C II is of considerable interest and importance for the accurate spectral analysis and astrophysical modeling. Over the last thirty years, a number of experiments and calculations have been performed for PI cross sections of C II. In theory, Yan *et al.*[12,13] calculated the PI cross sections and oscillator strengths of C II, as one of the first ions studied in the Opacity Project, for the states of valence excitations with the effective quantum number $n \leq 10$ and the total orbital angular momentum $L \leq 3$ in the close-coupling approximation, by using the R-matrix method described by Berrington *et al.*[14] These results have been revised by Lan *et al.*[15] and later, within the Iron Project, have been calculated by Nahar *et al.*[16] by using the same techniques such as those carried out within the Opacity Project, but a larger basis set and a finer energy resolution have been used. They also performed the calculations for the $C^{2+}+$ e recombination process (the inverse of the $C^+ + h\nu$ PI process) in the close-coupling approximation by using the R-matrix method.[17,18] In an experiment, Nicolosi and Recanatini *et al.*[19,20] measured the photoabsorption spectrum of the C II ion by the dual laser plasma technique. They obtained both the discrete spectrum with a series of resonance lines converging to the ionization threshold, and the relative PI cross sections above the first limit from the ground state $2s^22p(^2P^o)$

*Project supported by the National Key Research and Development Program of China (Grant No. 2017YFA0402300), the National Natural Science Foundation of China (Grant Nos. U1530142, 11474032, and 11774344), and the Young Teachers Scientific Research Ability Promotion Plan of Northwest Normal University (Grant No. NWNU-LKQN-15-3).

†Corresponding author. E-mail: xiely@nwnu.edu.cn

© 2018 Chinese Physical Society and IOP Publishing Ltd

and the excited state $2s2p^2(^4P^e)$. Kjeldsen *et al.*[21] reported the first absolute PI cross section with high accuracy by using a merged ion-photon beam setup with synchrotron radiation for C II for the region from threshold 24.38 eV up to 31 eV, where the photoionization of 2p valence electron and $2s^22p \rightarrow 2s2p(^3P^o)nl$ resonances are dominant. The extended experimental investigation has been performed subsequently by Kjeldsen *et al.*[22] to include photon energies up to 105 eV. Above 31 eV, the photoionization of the sub-shell 2s valence electron is dominant, the spectral structures are not as pronounced as in the threshold region, and some resonances from two-electron transitions are observed. There is generally, the experimental PI cross sections[21,22] and the various types of *R*-matrix calculations were in good agreement.[12,16] However, some important deviations are also observed both with respect to the continuum cross section and to the resonance structure. In particular, it is found that the observation of the $2s^22p^2P^o \rightarrow 2s2p(^3P)np^2P^e$ resonances cannot be predicted by those norelativistic calculations.[21,22] Using the Breit–Pauli *R*-matrix (BPRM) method, Nahar[24] performed detailed calculations for the PI cross section of the ground $2s^22p(^2P^o)$ and the excited $2s2p^2(^4P^e)$ states of C II near threshold and revealed the fine structure observed in the experiment, but his work was just limited to the photon energy region of 24 eV–31 eV. Therefore, the detailed relativistic *R*-matrix calculations are still needed for the region of higher photon energies (above 31 eV), where a difference of nearly up to 50% still exists between the experimental results and the previous calculations.

In this study, we perform comprehensive fully relativistic *R*-matrix calculations for the PI cross section of the ground state $2s^22p^2P^o_{1/2}$ and first excited state $2s^22p^2P^o_{3/2}$ state of CII using the Dirac atomic *R*-matrix code (DARC).[25] The attention mainly focuses on the *L*-shell (2p, 2s) photoionization for photon energy from the threshold (24.38 eV) up to 41.5 eV. The results are discussed and compared with early theoretical calculations and experimental measurements. In Section 2, the theoretical method and some computational details are briefly outlined. In Section 3, our calculations are presented and discussed. Finally, in Section 4, we draw some conclusions from the present study.

2. Theoretical method

The *R*-matrix method for electron-atom and photon–atom interactions has been discussed in great detail by Burke *et al.*[26] In this method, the Dirac Hamiltonian for the $(N+1)$-electron system can be written in atomic units as

$$H^{N+1} = \sum_{i=1}^{N+1} -\mathrm{i}c\boldsymbol{\alpha}\cdot\boldsymbol{\nabla}_i + (\beta-1)c^2 - \frac{Z}{r_i} + \sum_{j=i+1}^{N+1}\frac{1}{|\boldsymbol{r}_j-\boldsymbol{r}_i|}, \quad (1)$$

where i and j index the individual electrons, Z is the charge of an infinitely heavy point nucleus, the electron rest mass has been subtracted, and $\boldsymbol{\alpha}$ and β are the usual Dirac matrices constructed from Pauli spin and unit matrices. If the configuration space is partitioned into two regions separated by the *R*-matrix boundary R_a, the total wave function of the $(N+1)$-electron system in the internal region is given by[25]

$$\Psi_k^{N+1} = \sum_{ij'} c_{ij'k} A\left[\Phi_i^N, u_{ij'}\right]^{J\pi} + \sum_q d_{qk}\theta_q^{N+1}, \quad (2)$$

where k is the eigenvector index, i the channel index, j' the continuum basis function index, $A\left[\Phi_i^N, u_{ij'}\right]^{J\pi}$ the coupled wavefunction of the $(N+1)$-electron system with total angular momentum J and parity π, constructed from the N-electron target state wavefunction $\Phi_i^N = |J_i^t \pi_i^t\rangle$ and the basis functions for the continuum electron orbital $u = |\varepsilon\kappa m\rangle$, κ the relativistic angular quantum of a continuum electron, $\kappa = \pm(j+1/2)$ for $l = j \pm 1/2$, A the antisymmetric operator to account for the exchange effects between the target electrons and free electron, and θ_q^{N+1} the correlation function of $(N+1)$-electron system constructed by the square-integrable orbitals to account for the correlation effects not adequately considered because of the cutoff in the first sum, which is needed to make the wavefunction complete and orthogonalized. The boundary is chosen so that the magnitude of the radial spinor of the bound electrons of the target is vanishingly small, and the exchange between scattering electron and target electrons outside the *R*-matrix sphere is negligible. The coefficients $c_{ij'k}$ and d_{qk} are determined variationally, by diagonalizing the $(N+1)$-electron Dirac Hamiltonian matrix H^{N+1}.

The continuum wavefunctions are constructed from single-particle wavefunctions in the following form:[25]

$$|\varepsilon\kappa m\rangle = \frac{1}{r}\begin{pmatrix} P_{\varepsilon\kappa}(r) & \chi_{\kappa m}(\theta,\varphi) \\ \mathrm{i}Q_{\varepsilon\kappa}(r) & \chi_{-\kappa m}(\theta,\varphi)\end{pmatrix}, \quad (3)$$

where $P(r)$ and $Q(r)$ are the large and small component radial wave functions respectively, and $\chi_{\kappa m}$ is the spin-angular function.

In the present calculations, to generate the wavefunction of the $(N+1)$-electron system, the wavefunctions of the C III target state are described by 14 relativistic orbitals: $1s_{1/2}$, $2s_{1/2}$, $2p_{1/2}$, $2p_{3/2}$, $3s_{1/2}$, $3p_{1/2}$, $3p_{3/2}$, $3d_{3/2}$, $3d_{5/2}$, $4s_{1/2}$, $4p_{1/2}$, $4p_{3/2}$, $4d_{3/2}$, and $4d_{5/2}$. The GRASP2K package[27] based on the multiconfiguration Dirac–Fock (MCDF) method[28,29] is used to obtain these relativistic orbital wavefunctions. In the calculations, the $1s_{1/2}$, $2s_{1/2}$, $2p_{1/2}$, and $2p_{3/2}$ orbitals are treated as spectroscopic orbitals and optimszed by performing an extended optimal-level calculation for all levels from the configurations $1s^22s^2$, $1s^22s2p$, $1s^22p^2$, $1s2s^22p$, and $1s2p^3$, and the others are optmized as correlation orbitals with considering the additional configurations of $1s^22snl$ and $1s^22pnl$ ($n = 3, 4$; $l =$ s, p, d). There are a total of 38 configurations, namely $1s^22s^2$, $1s^22s2p$, $1s^22p^2$, $1s2s^22p$, $1s2s2p^2$, $1s2p^3$, $1s^23s^2$, $1s^23p^2$, and $1s^22snl$,

$1s^22pnl$, $1s2s^2nl$, $1s2p^2nl$, and $1s2s2pnl$ ($n = 3, 4$; $l =$ s, p, d) are included in the module DSTG2 of the DARC[25] to better describe the configuration interaction effects. The first 113 low-lying target states of them are incorporated to generate the possible PI channels and to obtain the wavefunctions of the $(N+1)$-electron system of C II. The R-matrix boundary radius is set to be 9.2 a.u. (atomic unit), which is sufficient to envelop all the $n = 2$ atomic orbitals of the residual C III ion, and thus ensuring that the wave function is completely wrapped within the R-matrix sphere. For each angular momentum, the continuum orbitals are expressed as a linear combination of 40 numerical basis functions. To resolve the fine resonant structure in the respective PI cross section, a suitably chosen fine energy mesh of 10^{-4} Ryd (1 Ryd = 13.6056923 eV) between the thresholds is adopted. Our calculated relativistic R-matrix target energies are shown in Table 1, and compared with previous R-matrix results of term energies calculated by Hasoglu *et al.*[30] and Wang *et al.*,[31] and the NIST values[32] for some valence- and core-excited states of C III ion. For valence-excited states, it is found that our results and others are in good agreement with each other. Our calculated energies accord well with NIST data within 2.18 percent and the maximum error appears for the excited state $1s^22p^2\ ^1S$. The energy levels calculated by Hasoglu *et al.*[30] are closer to the NIST values than ours and Wang *et al.*'s[31] calculations within 1.3 per cent except for the level $1s^22p^2\ ^1S$, where the difference is 2.36 percent. For core-excited states, there are no available NIST data for comparison. Our calculated energies are larger than those in Refs. [30] and [31], but the difference is less than 0.5%. The present calculated ionization potential (IP) values for the ground state $2s^22p\ ^2P^o_{1/2}$ and the first excited state $2s^22p\ ^2P^o_{3/2}$ are 1.7928 Ryd and 1.7921 Ryd respectively, they are in good agreement with the measured energies of 1.7921 Ryd and 1.7916 Ryd. The IP for the $2s^22p\ ^2P$ term is 1.7977 Ryd calculated by Hasoglu *et al.*[30] and 1.7843 Ryd calculated by Wang *et al.*[31]

Table 1. Calculated energies (in unit Ryd) for the target C III ion relative to the ground state $1s^22s^2\ ^1S_0$, and other available data in the literature,[30,31] with the NIST values for comparison.[32]

Config.	Term	$J^t\pi^t$	This	Ref. [30]	Ref. [31]	NIST[32]	Config.	Term	$J^t\pi^t$	This	Ref. [30]	Ref. [31]	NIST[32]
$1s^22s^2$	$^1S^e$	0 +					$1s2s(^1S)2p^2$	$^3P^e$	0 +	22.0673	21.9689	22.0311	
$1s^22s2p$	$^3P^o$	0 −	0.4759	0.4745	0.4781	0.4772			1 +	22.0677			
		1 −	0.4761			0.4774			2 +	22.0685			
		2 −	0.4766			0.4779	$1s2s(^3S)2p^2$	$^3D^e$	1 +	22.0919	21.9997	22.0359	
$1s^22s2p$	$^1P^o$	1 −	0.9530	0.9570	0.9446	0.9327			2 +	22.0920			
$1s^22p^2$	$^3P^e$	0 +	1.2690	1.2649	1.2549	1.2523			3 +	22.0921			
		1 +	1.2693			1.2526	$1s2s(^3S)2p^2$	$^1D^e$	2 +	22.4011	22.3201	22.3655	
		2 +	1.2698			1.2530	$1s2s(^3S)2p^2$	$^3S^e$	1 +	22.4130	22.3269	22.3157	
$1s^22p^2$	$^1D^e$	2 +	1.3525	1.3630	1.3401	1.3293	$1s2s(^3S)2p^2$	$^3P^e$	0 +	22.4877			
$1s^22p^2$	$^1S^e$	0 +	1.7615	1.7881	1.6823	1.6632			1 +	22.4882			
$1s^22s3s$	$^3S^e$	1 +	2.1619		2.1743	2.1708			2 +	22.4890			
$1s^22s3s$	$^1S^e$	0 +	2.2661		2.2519	2.2524	$1s2s(^3S)2p^2$	$^1P^e$	1 +	22.6677	22.5674	22.6143	
$1s^22s3p$	$^1P^o$	1 −	2.3747			2.3596	$1s2s(^1S)2p^2$	$^1S^e$	0 +	22.7249	22.6511	22.6449	
$1s^22s3p$	$^3P^o$	0 −	2.3777			2.3666	$1s2p^3$	$^5S^o$	2 −	22.4636		22.4255	
		1 −	2.3777			2.3667	$1s2p^3$	$^3D^o$	1 −	22.7497	22.6802	22.6956	
		2 −	2.3778			2.3668			2 −	22.7498			
$1s2s^22p$	$^3P^o$	0 −	21.4635	21.3622					3 −	22.7499			
		1 −	214640				$1s2p^3$	$^3S^o$	1 −	22.8781	22.7780	22.8319	
		2 −	21.4651				$1s2p^3$	$^1D^o$	2 −	22.9576	22.8708	22.9039	
$1s2s^22p$	$^1P^o$	1 −	21.6935	21.5849	21.6360		$1s2p^3$	$^3P^o$	0 −	23.0565	22.9926	22.9657	
$1s2s(^3S)2p^2$	$^5P^e$	1 +	21.5735		21.5283				1 −	23.0566			
		2 +	21.5740						2 −	23.0567			
		3 +	21.5748				$1s2p^3$	$^1P^o$	1 −	23.2669	23.1865	23.1750	

3. Results and discussion

The L-shell photonization processes for the ground state $2s^22p^2P^o_{1/2}$ and the first excited state $2s^22p\ ^2P^o_{3/2}$ of CII ion can be described in LSJ terms as

$$h\gamma + 2s^22p^2P^o_{1/2,3/2} \rightarrow \left\{2s^2(\text{or } 2s2p) + e^-(\varepsilon l)\right\}{}^2S^e_{1/2}, {}^2P^e_{1/2,3/2}, {}^2D^e_{3/2,5/2}. \quad (4)$$

Here, for the $^2P_{1/2}$ ground state, according to the dipole selection rules, the following three partial transitions: $^2P^o_{1/2} \rightarrow {}^2S^o_{1/2}$, $^2P^o_{1/2,3/2}$, $^2D^o_{3/2}$ are required, which satisfy the two J^π symmetries $1/2^o \rightarrow 1/2^e, 3/2^e$. For the $^2P_{3/2}$ state, it contains five partial transitions: $^2P^o_{3/2} \rightarrow {}^2S^e_{1/2}$, $^2P^e_{1/2,3/2}$, and $^2D^e_{3/2,5/2}$, which satisfy the three J^π symmetries $3/2^o \rightarrow 1/2^e, 3/2^e, 5/2^e$.

Figure 1(b) shows the calculated total PI cross section of the states $2s^22p^2P^o_{1/2}$ (solid curve) and $^2P^o_{3/2}$ (dashed curve) of CII in the near threshold regions, namely 24 eV–31 eV of photon energy. As a comparison, the nonrelativistic *R*-Matrix results for the ground term $2s^22p(^2P^o)$ obtained by Nahar[16] in *LS* coupling are plotted in Fig. 1(a). It is found that the fine structure features are different and more extensive resonance structures are introduced due to automatically including the relativistic effects (mainly the spin–orbital and spin-spin interactions) in the present calculations, besides the resonance positions that have about 0.047 eV minor shifts toward lower energy when compared with the nonrelativistic calculations.[16] The cross section in regions below 2s2p $^3P^o$ limit (30.88 eV)[22] is mainly characterized by $2s \rightarrow np$ resonances embedded in continua of the type $2p \rightarrow \varepsilon l$ transition. The most distinct resonances observed in Figs. 1(a) and 1(b) should be due to $2s^22p^2P^o \rightarrow 2s2p(^3P)np\ ^2P^e$, $^2D^e$, and $^2S^e$ transitions ($n \geq 4$). For a given autoionizing resonance configuration, such as $2s2p(^3P)4p$ complex, the first three resonances in cross section belong to the $2s2p(^3P)4p\ ^2P^e$, $^2D^e$ and $^2S^e$ states respectively in Fig. 1(b), and the fourth resonance, which can be identified as the combination of the $2s2p(^1P)4p\ ^2P^e$, $^2D^e$, $^2S^e$ states, is common for the whole Rydberg series. It is obvious that the $2s^22p^2P^o \rightarrow 2s2p(^3P)np\ ^2P^e$ resonances are not predicted by the non-relativistic calculations in Nahar's work[16] (Fig. 1(a)), because the autoionizing states $2s2p(^3P)np\ ^2P^e$ cannot decay via a radiationless transition to the $2s^2(^1S)\varepsilon l$ continuum with the same symmetry $^2P^e$, but are allowed in relativistic intermediate coupling. Figure 1(c) displays that the present relativistic PI cross sections after the convolution of the calculated resonance with a Gaussian distribution function of the full width at half maximum (FWHM) of 35 meV representing the instrumental resolution, are compared with the measured absolute PI cross sections of CII (see Fig. 1(d)) by Kjeldson *et al.*[21,22] by using a merged ion-photon beam setup with synchrotron radiation. It is found that, in general, the resonance features of the present calculations (Fig. 1(c)) and the experimental results (Fig. 1(d)) are in very good agreement. However, some differences are also noted for the higher resonance complexes, and the calculated continuum cross section is approximately 10% larger than the measurement. The PI cross sections for the levels of the ground state $2s^22p^2P^o_{1/2,3/2}$, and of the metastable state

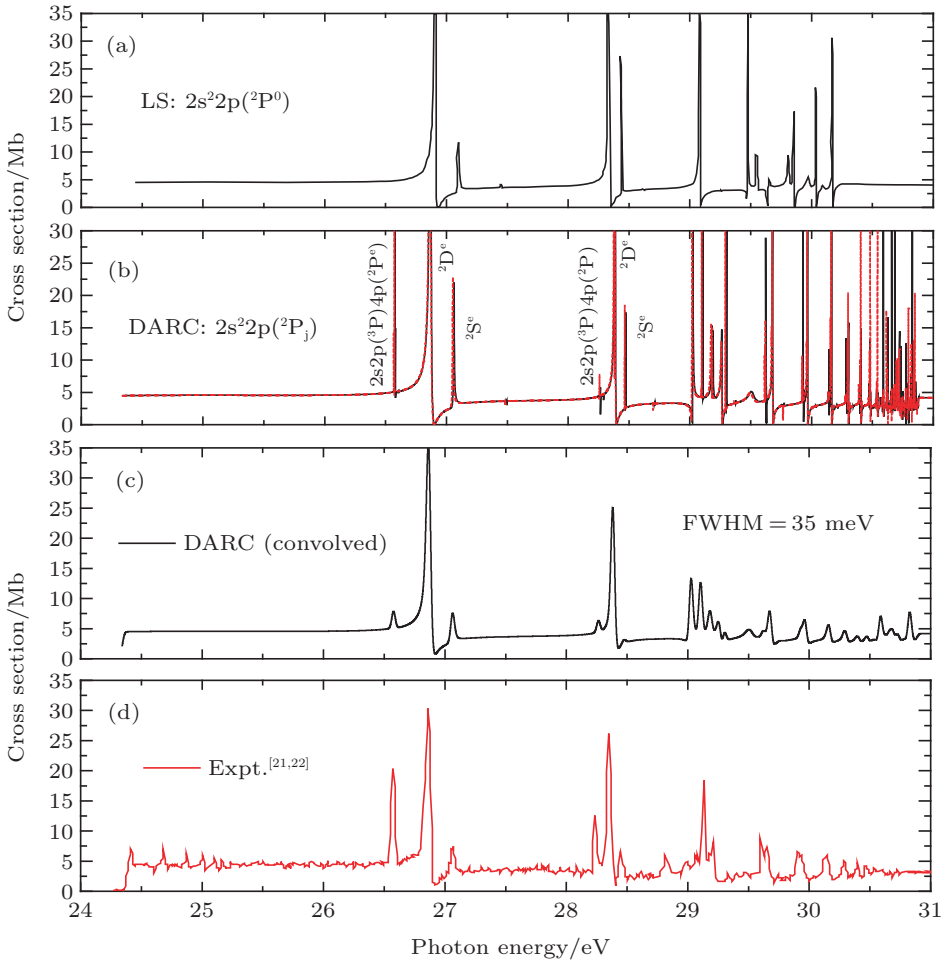


Fig. 1. (color online) Photoionization cross sections of CII from the photon energy region 24 eV–31 eV. (a) Nonrelativistic *R*-Matrix results for ground term $2s^22p\ (^2P^o)$ in *LS* coupling by Nahar;[16] (b) DARC results for fine structure levels of the ground state $2s^22p\ ^2P^o_{1/2}$ (solid curve) and the first excited state $^2P^o_{3/2}$ (dashed curve); (c) present theoretical data convolved with a Gaussian FWHM of 35 meV; (d) experimentally measured cross sections by Kjeldsen *et al.*[21,22] The unit 1 barn = 10^{-24} cm^2.

$2s2p^2{}^4P^e_{1/2,3/2,5/2}$ of CII in the region 24 eV–31 eV have also been calculated by Nahar[24] including 20 fine-structure levels target states by using the BPRM method. The present results are in good agreement with the BPRM calculations by Nahar[24] for the $2s^22p^2P^o_{1/2,3/2}$ states. It demonstrates that the relativistic effects should be incorporated into the PI cross section calculations, even for light atomic systems, such as C II.

Figures 2(a) and 2(b) show the partial and total PI cross sections for the fine structure levels of $2s^22p^2P^o_{1/2}$ and $^2P^o_{3/2}$ in the region 31.4 eV–37.4 eV, where the photon energies are above the $2s2p^3P^o$ limit (30.88 eV), and the $2s \rightarrow np$ resonances, and $2s \rightarrow \varepsilon l$ continua phtoionization spectrum is dominated. For the $2s^22p^2P^o_{1/2}$ level, the partial cross section from the $J^\pi = 3/2^e$ transition contributes most to the total PI cross section, while for the $2s^22p\ ^2P^o_{3/2}$ state, the most important partial cross section is due to the $J^\pi = 5/2^e$ transition, and the partial cross sections, which come from $J^\pi = 1/2^e$ and $3/2^e$, are also important for the resonances. In Fig. 2(c), we compare the total cross sections for the $2s^22p^2P^o_{1/2}$ and $^2P^o_{3/2}$ levels; it is found that both the continuum and resonance features are very similar for those two states because of the very small split of the energy, though the partial cross sections are quite different for them. Thus, it demonstrates that the influences of relativistic effects on PI cross sections of different fine structure levels derive from the same term $2s^22p^2P^o$ in CII are small and can be neglected.

In Fig. 3, the averaged total PI cross sections for the $2s^22p\ ^2P^o$ state are compared with the measured cross sections by Kjeldson *et al.*,[21,22] together with the nonrelativistic cross sections by Nahar *et al.*[16] In the experiment by Kjeldson *et al.*,[21,22] in addition to the C II $2s^22p^2P^o$ ground state, there was also a 5% $2s2p^2(^4P^e)$ metastable-state fraction giving additional resonances not included in our calculations. The theoretical cross sections by Nahar *et al.*[16] have been convoluted with Gaussian distribution functions of FWHM of 55 meV representing the instrumental resolution in Ref. [21]. To resolve the more detailed resonances of the measurements, the FWHM of 40 meV was taken into account in the present calculations. From Fig. 3, we can find that the position of the resonance and the intensity of the peak obtained from the present calculations and their corresponding measurements are in good agreement. In particular, we note that the observed double peaks due to the transitions $2s^22p^2P^o \rightarrow 2s2p(^1P^o)5p\ ^2D^e_{3/2,5/2}$, $^2P^e_{1/2,3/2}\ ^2S^e_{1/2}$ are clearly revealed in the present calculations, which have not been shown in the results of Nahar *et al.*[16] By analyzing the partial transition contributions to the total photoionization cross section for the states $2s^22p^2P^o_{1/2}$ and $^2P^o_{3/2}$, respectively, we find that detailed resonant structures of the observed double peaks are associated with the $2s2p(^1P)5p^2D^e_{3/2;5/2}$ autoionizing state in lower energy, and the $2s2p(^1P)5p^2P^e_{1/2;3/2}$ autoionizing state in higher energy. The resonance from the $2s2p(^1P)5p^2S_{1/2}{}^e$ autoionizing state is very weak compared with those from $^2D^e_{3/2,5/2}$ and $^2P^e_{1/2;3/2}$, so it cannot be observed in the experimental PI spectra. For the other $2s^22p^2P^o \rightarrow 2s2p(^1P)np$ $n \geq 6$ Rydberg series, the situation is similar to the scenario for the transition $2s^22p^2P^o$-$2s2p(^1P)5p\ ^2D^e_{3/2,5/2}$, $^2P^e_{1/2,3/2}\ ^2S^e_{1/2}$, but the double peaks are not very obvious, especially for the higher-n Rydberg series. The resonances from the $2s2p(^1P)4p^2D^e_{3/2,5/2}$ and $^2P^e_{1/2;3/2}$, $^2S^e_{1/2}$ in Fig. 3 show broader features than from the other members of $2s^22p^2P^o$-$2s2p(^1P)np$ resonance series. Besides the above mentioned resonances from the one-electron transitions, the two-electron transitions of $2s^22p^2P^o \rightarrow 2p^2(^3P)3s$, $2p^2(^3P)3d\ ^2P^e$, $^2D^e$, $^2S^e$ are also very prominent in the region 31 eV–37 eV of photon energy. It should be noted that our results are still approximately 20% larger than the measured absolute PI cross sections in the region, whereas their agreement is good near the threshold.

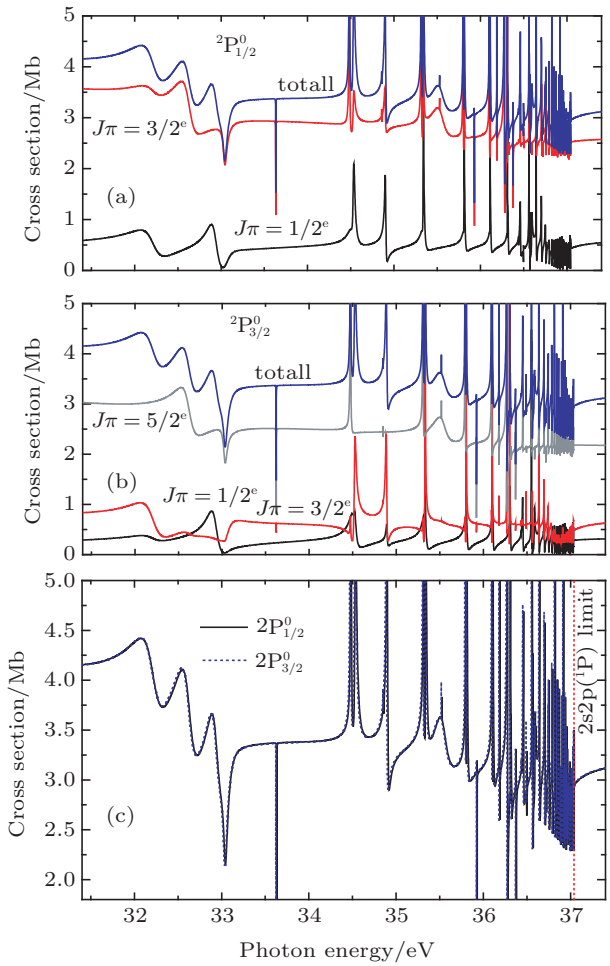


Fig. 2. (color online) Partial and total photoionization cross section of the $2s^22p\ ^2P^o_{1/2}$ and $^2P^o_{3/2}$ states of C II from the region 31.4 eV–37.4 eV (a) for the $^2P^o_{1/2}$ state, (b) for the $^2P^o_{3/2}$ state; (c) comparison of the total cross sections between $^2P^o_{1/2}$ (solid curve) and $^2P^o_{3/2}$ (dotted curve).

The PI cross section of the $2s^22p^2P^o_{1/2}$ and $^2P^o_{3/2}$ of C II in the region 36.5 eV–41.5 eV are shown in detail in Fig. 4. The

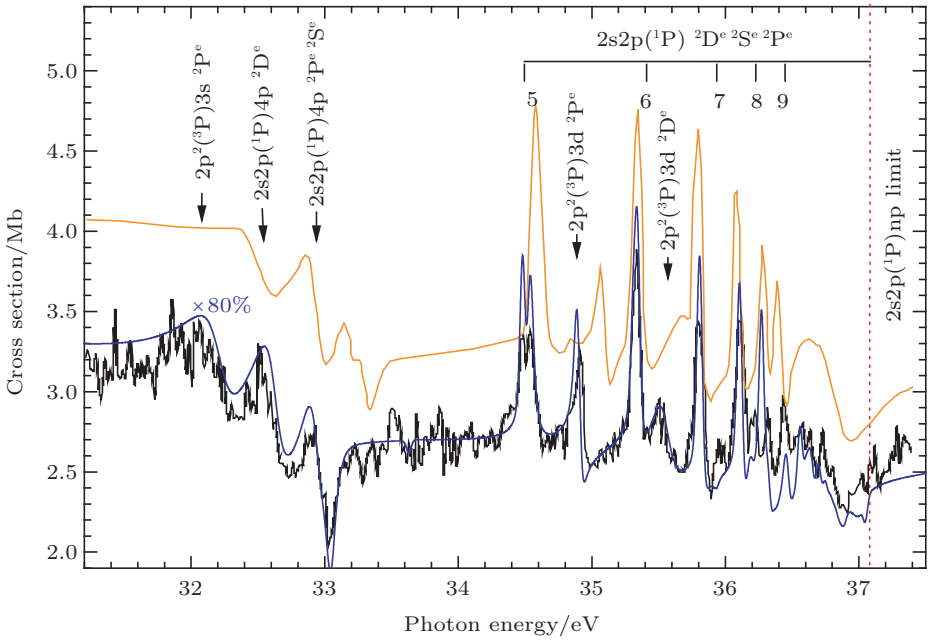


Fig. 3. (color online) Total photoionization cross section of the $2s^2 2p\ ^2P$ term of CII from the region 31.4–37.4 eV. Solid black curve: experimental data measured by Kjeldsen *et al.*;[22] solid blue curve: the present data convolved with a Gaussian FWHM of 40 meV and multiplied by 0.8; solid gray curve: norelativistic *R*-matrix results by Nahar.[16]

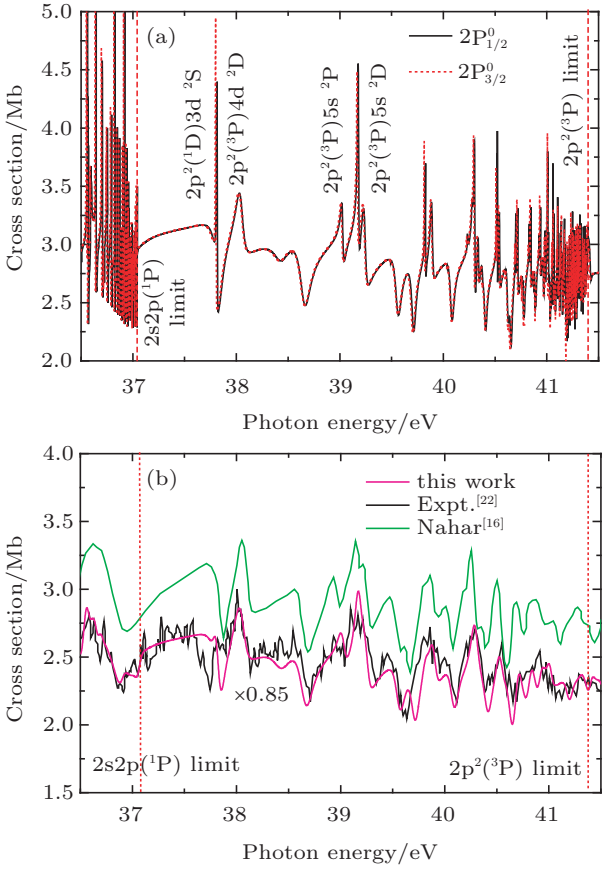


Fig. 4. (color online) PI cross section of the ground state $2s^2 2p\ ^2P^o_{1/2}$ and the excited state $^2P^o_{3/2}$ of C II ions from the region 36.5 eV–41.5 eV of photon energy, showing (a) detailed resonances for the ground state $^2P^o_{1/2}$ (solid curve) and the excited state $^2P^o_{3/2}$, (b) theoretical data convolved with Gaussian FWHM of 40 meV and multiplied by 0.85 (magenta line), and compared with experimentally measured cross sections (black line) by Kjeldsen *et al.*[22] and norelativistic *R*-matrix results (green line) by Nahar.[16]

resonance peaks in the region are dominated by two-electron transitions, which are more difficult to calculate and to identify. We only identify a few of them following the CI calculations performed by Kjeldson *et al.*[22] The relativistic cross section for the levels $^2P^o_{1/2}$ and $^2P^o_{2/3}$ show many overlapping resonances. The main resonance structures above the $2s2p(^1P)$ limit are due to $2s^2 2p^2 P^o \rightarrow 2p^2(^1D)nd$, $2p^2(^3P)ns$, nd transitions, which mix together, thus complicating the analysis. Comparing the present convolved cross sections with experimentally measured cross sections by Kjeldsen *et al.*[22] and norelativistic *R*-matrix calculations by Nahar,[16] good agreement is obtained for the resonance peaks both in positions and shapes, but the calculations predict that the cross section is 15% larger than the experimental values.

4. Conclusions

Using the fully relativistic *R*-Matrix code DARC, we have calculated the *L*-shell (2p, 2s) photoionization cross section of the ground state $2s^2 2p^2 P^o_{1/2}$ and the first excited state $2s^2 2p^2 P^o_{3/2}$ of C II ions. It is found that the relativistic effects are very important even for light atomic systems such as C II, which account for nearly all experimentally observed resonant features that may not be obtained in the nonrelativistic *LS* coupling calculations. The present fully relativistic results agree with the relativistic BPRM calculations and reveal the fine structure observed for the experimental measurement of near the threshold PI cross sections. Good agreement is also found between our results and the experimental resonance peaks for the inner 2s subshell PI cross sections, however, there are still about 10%–20% deviations observed for the continua phtoion-

ization spectra that need to be further studied in the future.

References

[1] Gao L C, Zhang D H, Xie L Y, Wang J G, Shi Y L and Dong C Z 2013 *J. Phys. B: At. Mol Opt. Phys.* **46** 175402
[2] Li C Y, Han X Y, Wang J G and Qu Y Z 2013 *Chin. Phys. B* **22** 0123201
[3] Davidson K 1972 *Astrophys. J.* **171** 213
[4] Colgan J, Zhang H L and Fontes C J 2008 *Phys. Rev. A* **77** 062704
[5] Nazir R T, Bari M A, Bilal M, Sardar S, Nasim M H and Salahuddin M 2017 *Chin. Phys. B* **26** 023102
[6] Seaton M J 1987 *J. Phys. B: At. Mol. Opt. Phys.* **20** 6363
[7] The Opacity Project Team 1995 *The Opacity Project*, Vol. 1 (Bristol, UK: Institute of Physics Publishing)
[8] Hummer D G, Berrington K A, Eissner W, Pradhan A K, Saraph H E and Tully J A 1993 *Astron. Astrophys.* **279** 298
[9] Berrington K A and Balance C 2001 *J. Phys. B: At. Mol. Opt. Phys.* **34** L383
[10] Kjeldsen H 2006 *J. Phys. B: At. Mol. Opt. Phys.* **39** R325
[11] Müller A, Schippers S, Phaneuf R A, Kilcoyne A L D, Bräuning H, Schlachter A S, Lu M and McLaughlin B M 2010 *J. Phys. B: At. Mol. Opt. Phys.* **43** 225201
[12] Yan Y and Seaton M J 1987 *J. Phys. B: At. Mol. Opt. Phys.* **20** 6409
[13] Yan Y, Taylor K T and Seaton M J 1987 *J. Phys. B: At. Mol. Opt. Phys.* **20** 6399
[14] Berrington K A, Burke P G, Dufton P L and Kingston A E 1977 *J. Phys. B: At. Mol. Opt. Phys.* **10** 1465
[15] Lan V K, Dourneuf M L, Allard N L, Saraph H E and Eissner W 1989 *Comput. Phys. Commun.* **55** 303
[16] Nahar S N and Pradhan A K 1997 *Astrophys. J. Suppl.* **111** 339
[17] Nahar S N 1995 *Astrophys. J. Suppl.* **101** 423
[18] Nahar S N and Pradhan K A 1994 *Phys. Rev. A* **49** 1816
[19] Nicolosi P and Villoresi P 1998 *Phys. Rev. A* **58** 4985
[20] Recanatini P, Nicolosi P and Villoresi P 2001 *Phys. Rev. A* **64** 012509
[21] Kjeldsen H, Folkmann F, Hansen J E, Knudsen H, Rasmussen M S, West J B and Andersen T 1999 *Astrophys. J.* **524** L143
[22] Kjeldsen H, Hansen J E, Folkmann F, Knudsen H, West J B and Andersen T 2001 *Astrophys. J. Suppl.* **135** 285
[23] Berrington K A, Eissner W and Norrington P H 1995 *Comput. Phys. Commun.* **92** 290
[24] Nahar S N 2002 *Phys. Rev. A* **65** 052702
[25] Norrington P H 2004 http://www.am.qub.ac.uk/DARC.
[26] Burke P G and Berrington K A 1993 *Atomic and Molecular Processes: An R-Matrix Approach* (Bristol, UK: Institute of Physics Publishing)
[27] Jönsson P, He X, Fischer C F and Grant I P 2007 *Comput. Phys. Commun.* **177** 597
[28] Grant I P 2007 *Relativistic Quantum Theory of Atoms and Molecules* (New York: Springer)
[29] Jönsson P, Parpia F A and C F Fischer 1996 *Comput. Phys. Commun.* **96** 301
[30] Hasoglu M F, Abdel-Naby Sh A, Gorczyca T W, Drake J J and McLaughlin B M 2010 *Astrophys. J.* **724** 1296
[31] Wang L G and Zhou X X 2007 *Chin. Phys.* **16** 2361
[32] Kramida A, Ralchenko Yu, Reader J and NIST ASD Team 2018 NIST Atomic Spectra Database (ver. 5.5.3), [Online] Available: https://physics.nist.gov/asd